In-situ TEM of Carbon Nanotube Field Emitters and Improvement of Electron Emission from Nanotube Films by Laser Treatment

Yahachi Saito, Kazuyuki Seko and Jun-ichi Kinoshita
Dept. of Quantum Engineering, Nagoya University, Chikusa-ku, Nagoya 464-8603, Japan
Toshiyuki Ishida
THE JAPAN STEEL WORKS, LTD., 2-2-1 Fukuura, Kanazawa-ku, Yokohama 236-0004, Japan
Junko Yotani, Hiroyuki Kurachi and Sashiro Uemura
NORITAKE CO., LTD., 728-23 Tsumura-cho, Ise 516-1103, Japan

Abstract
Dynamic behavior of carbon nanotubes (CNTs) in an electric field is directly observed by in-situ transmission electron microscopy (TEM). The CNT field emitters examined by in-situ TEM are multi-walled, double-walled and single-walled CNTs. Threshold fields for electron emission and sustainable emission currents depending on the structure of CNTs are presented, and degradation mechanism of the CNT field emitters is discussed. In addition to the microscopy studies on individual CNTs, our recent development in surface treatment of CNT layers grown by chemical vapor deposition, which brings about high density of emission current and high uniformity, is also presented.

1. Introduction
Carbon Nanotubes (CNTs) have been attracting considerable attention as field emitters because of their excellent properties such as high aspect ratio, high mechanical strength and high chemical stability. At present, researches for practical application of CNTs as field emitters in field emission displays (FEDs) are very active[1-4]. High current density, emission stability and uniformity are required for electron emitters in FEDs. In order to realize the structures of CNTs themselves as well as textures of a CNT assembly that are appropriate for field emitters, it is indispensable to examine directly the behavior of CNT emitters in an electric field and to elucidate their aging process and degradation mechanism. Wei et al. [5] for the first time reported the stability and failure of field-emitting multi-wall carbon nanotubes (MWNTs) using in-situ scanning electron microscopy (SEM). Wang et al. [6], using in-situ transmission electron microscopy (TEM), observed strong field-induced structural damage of MWNTs.
Fabrication of CNT cathodes for FEDs has been pursued mainly by two methods; one is screen printing of CNT-bearing past and the other is direct growth of CNT by chemical vapor deposition (CVD). In either method, surface treatment is necessary to activate or improve the emission properties.
In this paper, we report direct observation of field-emitting CNTs by-situ TEM. CNTs examined include a closed-cap multiwall CNT (MWNT), an open-ended MWNT, and double-wall carbon nanotubes (DWNTs) and single-wall CNTs (SWNTs). In addition to the in-situ TEM of CNT emitters, a surface treatment of CNT cathodes by laser irradiation which brings about high emission current and high uniformity of electron emission is also reported.

2. In-situ TEM for Direct Observation of CNT emitters
2.1 Preparation of CNT Emitters
CNTs used for the in-situ TEM were MWNTs, bundles of DWNT, and bundles of SWNTs, all of which were produced by arc discharge [7]. The diameters of a MWNT, a DWNT and a SWNT were 5-10 nm, about 4 nm and 1.3 nm, respectively. CNTs were fixed at the tip of a tungsten (W) needle by electrophoresis as follows. CNTs were suspended in distilled water by sonication, and a droplet containing CNTs was placed on a copper plate. The W needle, which was prepared by electrolytic polishing, was dipped into the droplet on the copper plate. An AC electric voltage of 10 V (5 MHz) was applied between the W needle and the copper plate to induce the electrophoresis as shown in Fig. 1 (a). The CNTs fixed on the W tip formed a bundle consisting of from several CNTs for MWNTs to tens of CNTs for SWNTs, as shown in Fig. 1 (b).

CNT emitters (cathode) and a copper plate (anode) were held on a special sample holder of TEM [8]. The anode stage allows 3-dimensional motion by a

piezoelectric drive, while the cathode stage is a fixed stage. The distances between the CNT cathode and copper anode were typically 1.2 - 2.0μm. The DC voltage between the CNT emitter and the copper anode was raised from 50 V up to 100 V at a rate of 0.28 V/s, and then reduced to 50 V at the same rate.

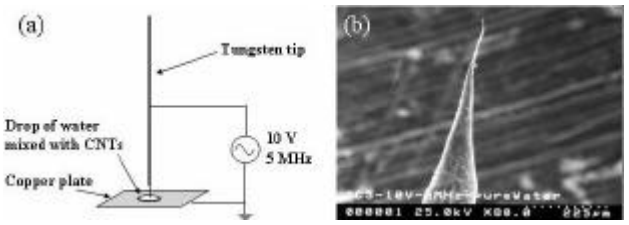

Fig. 1. (a) Schematic of the electrophoresis for fixing CNTs to a tungsten tip, (b) SEM image of a bundle of CNTs sticking out from the W tip.

2.2 Closed-capped MWNT

TEM images of closed MWNTs before and after the field emission (FE) experiment are shown in Figs. 2 (a) and (b), respectively. The tip of the MWNTs was attached to the anode surface gently in order to avoid a mechanical vibration of the tip. Two MWNTs were adhered with each other in parallel. The thick MWNT had a diameter of about 6 nm, and the number of layers was five at its tip part. The FE experiment was carried by raising electric voltage from 50 V up to 100 V and then by reducing to 50 V.

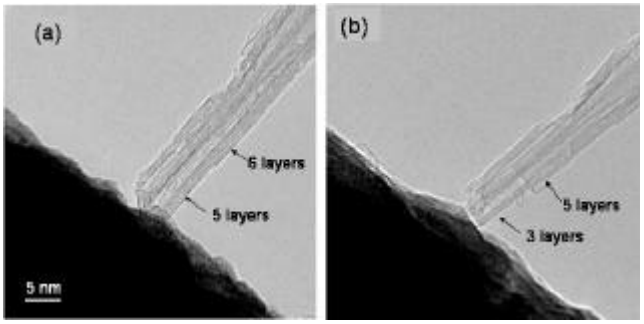

Fig. 2. TEM images of a closed MWNT (a) before and (b) after field emission.

experiment revealed that the number of graphene layers at the tip was reduced to three, as shown in Fig. 2 (b), indicating sublimation of two layers. The *I-V* curve (Fig. 3) shows that in a course of reducing voltage the emission current in a region below 70 V was higher than that before the sublimation of two layers. This increase in the emission current after the removal of layers may be caused by an increased field concentration due to the sharpened tip.

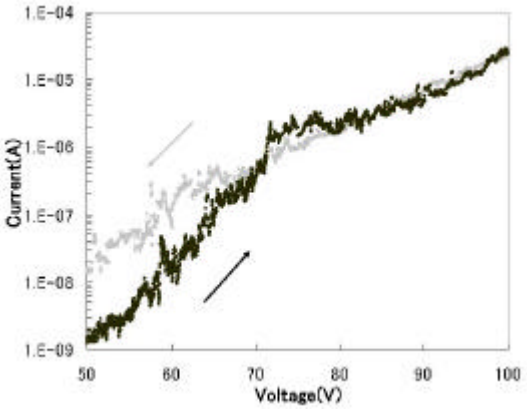

Fig. 3. *I-V* characteristics for the closed-cap MWNTs emitter.

2.3 Open-ended MWNT

An open-ended MWNT was fabricated from a close-ended MWNT by electrically attacking the tip in the TEM. Figure 4 (a) shows a TEM image of an open MWNT during FE at 80 V. The tip of the MWNT

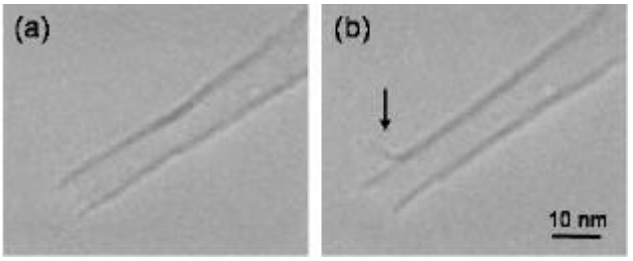

Fig. 4. TEM images of the open MWNT under FE (a) at 80 V and (b) at 86 V.

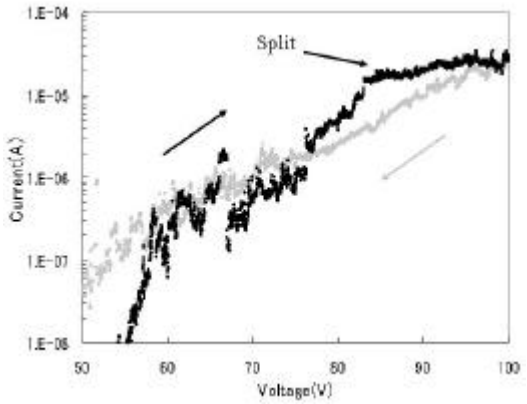

Fig. 5. *I-V* characteristics corresponding to the open MWNT shown in Fig. 4

consisted of several layers. The diameter of the MWNT at the tip was 9 nm. The outer layer at the tip of MWNT peeled off about 8 nm in length and at the applied voltage of 86 V, as shown in Fig. 4 (b). The split layer then sublimated at 93 V. Finally, the tip of the MWNT sublimated over a length of 150 nm at 98 V. The *I-V* characteristics of the open MWNT emitter is shown in Fig.5. Maximum emission current was 34 μA at 96 V after the sublimation of the peeled layer.

2.4 Bundle of DWNTs

TEM images of DWNT emitters during FE are shown in Fig.6. DWNTs in the present study formed bundles, each of which consisted of several to ten DWNTs. A bundle of DWNTs (arrow A in Fig. 6 (b)) split off like a "Y" shape at about 60 V. When the voltage was raised from 60 V to 85 V, the protruding bundle (A) in Fig. 6 (b) shortened gradually (see Figs. 6 (c) and (d)). The total length the bundle A lost was about 1.6 μm for 144 sec (Figs.6 (c) and (d)). A broken line in Fig.6 (e) traces an equal distance from the anode surface. Protruding bundles failed one after another from the nearest bundle to the anode surface. Finally, the shortening of a DWNT bundle stopped when the distance from the anode surface to the tip of a bundle became approximately equal to that for neighboring bundles as observed in Fig. 6 (e), in which a broken line traces an equal distance from the anode surface. The *I-V* characteristics of the DWNTs (Fig. 6) are shown in Fig.7. Sublimation of protruding bundles was observed in the voltage region indicated by a broken line with arrows. A sudden decrease in the current at 84 V corresponds to shortening of the protruding bundle with a split tip (arrow A in Figs. 6 (c) and (d)). Just before the sudden decrease, the maximum emission current was 12 μA, and after the sublimation, the current reduced to 2 μA. Thus, it is considered that the sublimated bundle sustained emission current of 10 μA. Since one bundle contains about seven DWNTs, the maximum sustainable current per a single DWNT is calculated to be 1.7 μA. As revealed in Fig. 7, further increase in voltage brought about a sudden increase in current at the voltage 95 V, where splitting of another bundle (arrow B in Fig. 6) occurred. This sudden increase in emission current is attributable to the splitting of the tip of the DWNT bundle. In a course of decreasing voltage, the emission current did not recovered to its original value due to the degradation of the DWNT emitters.

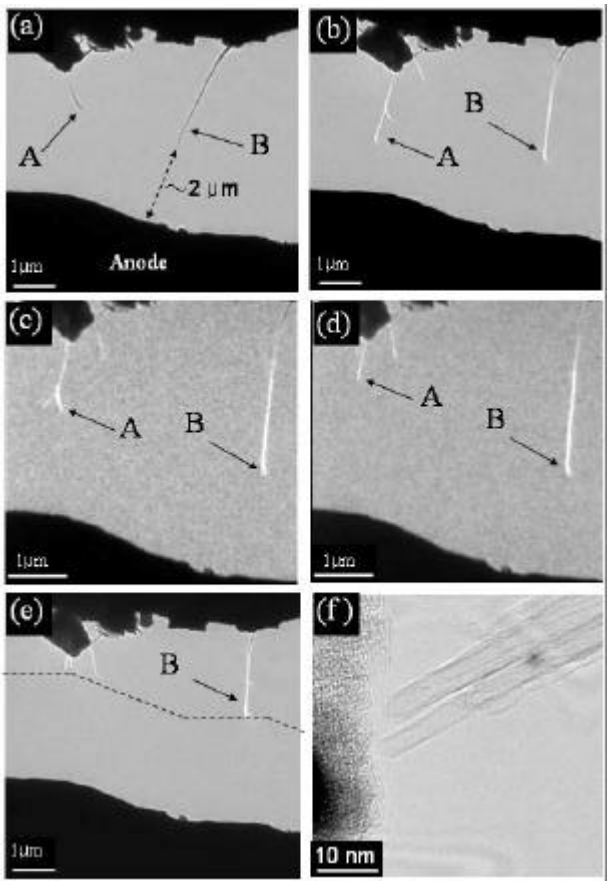

Fig. 6. A series of TEM images of DWNT bundles under various applied voltages. (a) 0 V, (b) 60 V, ~ 2.5 μA, (c) 70 V, ~ 6.0 μA, (d) 85 V, ~ 2.0 μA, (e) 100 V, ~ 13.0 μA. (f) High-resolution TEM images of a DWNT bundle after the FE experiment.

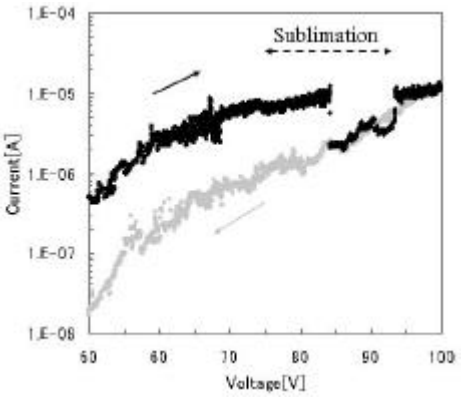

Fig. 7. *I-V* characteristics corresponding to the FE experiment of Fig.6. In a voltage region indicated by the broken line with arrows, the protruding bundle shortened.

2.4 Bundle of SWNTs

Figure 8 (a) shows a TEM image of a bundle of SWNTs attached on the tip of the W needle before FE experiment. The bundle began week vibration when 50 V was applied, and it suddenly began intense oscillation at 60 V (Fig.8 (b)). The bundle finally disrupted at 70 V, and the disrupted bundle is shown in Fig. 8 (c). Figure 8 (d) shows the *I-V* characteristics before and after the break of the bundle. The three regions (I), (II), and (III) correspond to the weak and intense vibration, and after the breakage, respectively. This intense vibration occurred only occasionally, while the weak vibration occurred frequently.

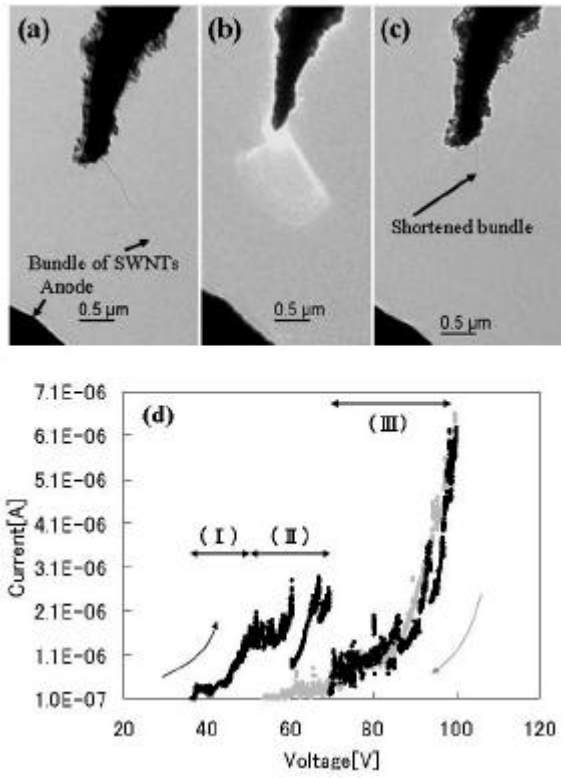

Fig. 8 TEM images of a SWNT bundle at various applied voltages (a) 0 V, (b) 62 V, and (c) 0 V after the violent vibration. The bundle began to vibrate violently at 62 V and it was broken finally at 69 V. (d) *I-V* characteristics before and after the break of the bundle

3. Threshold Electric Field and Sustainable Current Density for Various CNTs

Table I summarizes emission characteristics of the four types of CNTs; close-ended and open-ended MWNTs, DWNTs and SWNTs. E_{th}, and J_{sub} are defined as follows; E_{th} is a macroscopic threshold electric field $E_{th} = V/d$ required for emission current of 1 μA, where V is the applied voltage and d is the distance from the tip of the field emitter to the surface of the counter electrode, and J_{sub} is current density for initiating sublimation. C-MWNT and O-MWNT represent the closed MWNT and open MWNT, respectively. J_{sub} of the open MWNT emitter is nearly equal to that of the close MWNT. On the other hand, though the SWNTs has the lowest E_{th} and E_{hc}, they are the most easily degraded (J_{sub} is the lowest). DWNTs are between the MWNT and SWNT in respect of the threshold voltage and the sustainable current.

Table 1 Threshold electric fields required for 1μA and sustainable current density for various CNTs

	O-MWNT	C-MWNT	DWNTs	SWNTs
E_{th} (at I_E = 1μA) [V/μm]	60	60	54	45
J_{sub} [10^7 A/cm^2]	6.6	5.2	1.4	0.4

In our experiment, the maximum emission current just before sublimation was 1.7 μA per a single DWNT. It was reported that the temperature at a tip of MWNT under FE was raised to 2000 K when the emission current was 1.2 μA [9]. So, the degradation of the present CNT field emitters is presumably due to thermal evaporation by Joule heating at the tip of the bundle. C-MWNTs were the most robust against degradation though the threshold voltage was the highest. O-MWNTs were more apt to degrade than the closed ones. SWNTs showed the lowest threshold voltage but were the most easily degraded. DWNTs showed the between MWNTs and DWNTs in the robustness and the easy in FE. Degradation and failure of the present CNT field emitters is presumably due to thermal evaporation by Joule heating at the tip of the bundle.

4. Emission Enhancement of Web-Like CNT Cathodes by Laser Irradiation

4.1 Preparation of Web-Like CNT Cathodes

A layer of CNTs was directly grown on surface of a metal electrode made of 426-alloy (42 wt%Ni, 6 wt%Cr, balance-Fe) by thermal-CVD with CO as carbon feedstock and H_2 as carrier gas [10]. Catalyst elements necessary for CNT growth are included in

the alloy. The metal electrodes (11.8 mm in diameter and 0.1 mm in thickness) had hexagonal holes (length of hexagon edge was 200 μm) in a honeycomb pattern (approximately 55 holes per inch).

Scanning electron microscopy (SEM) revealed that the electrode surface was conformably covered with a CNT layer, i.e., the edges and the surfaces were smoothly covered. High-magnification SEM showed that the CNTs form a web-like network structure (Fig. 9). The thickness of the CNT layer was approximately 15 μm. TEM revealed that the CNTs grown by this method were multiwalled CNT with diameter of 26 nm in average.

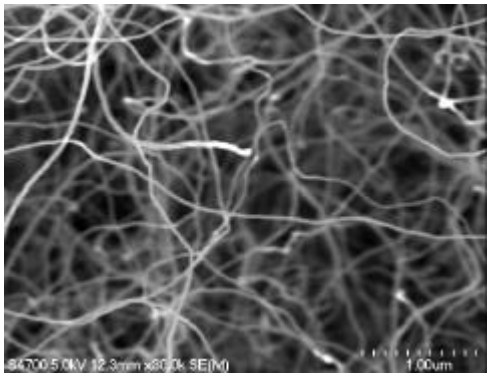

Fig. 9. SEM image of surface of the CNT layer before laser irradiation.

4.2 Surface Treatment by Laser Irradiation

Surface treatment of the CNT cathode was carried out with a laser irradiation apparatus developed by THE JAPAN STEEL WORKS. A KrF excimer laser (248nm) with repetition frequency 20 Hz and pulse width 20ns was used. Laser spot area with uniform intensity was expanded to 8 mm × 8 mm by a special optics. Laser energy density was adjusted from 30 mJ/cm^2 to 110 mJ/cm^2, and the laser irradiated the center of specimen with 3 shots in air. *I-V* characteristics and electron-emission distribution over the CNT cathode were measured by using a cathode emission profiler (Tokyo Cathode Laboratory) [11].

4.3 Field Emission from Laser-Treated CNT Cathodes

TEM revealed that the tips of CNTs were opened by laser irradiation of 50 mJ/cm^2 and had sharp edges like a point of a hypodermic needle, though most of CNT tips before irradiation were capped including catalyst particles. Number of tips created by laser irradiation increased with the increase of laser energy density: 5 x 10^7/cm^2 for 30 mJ/cm^2 and 1.7 x 10^8/cm^2 for 90 mJ/cm^2. In the case of laser irradiation of 50 mJ/cm^2, tips of CNTs were observed to be randomly distributed throughout the networked CNT structure, while in case of 90 mJ/cm^2 the networked CNT structure was seriously damaged and the tips of CNTs were observed to be gathered together.

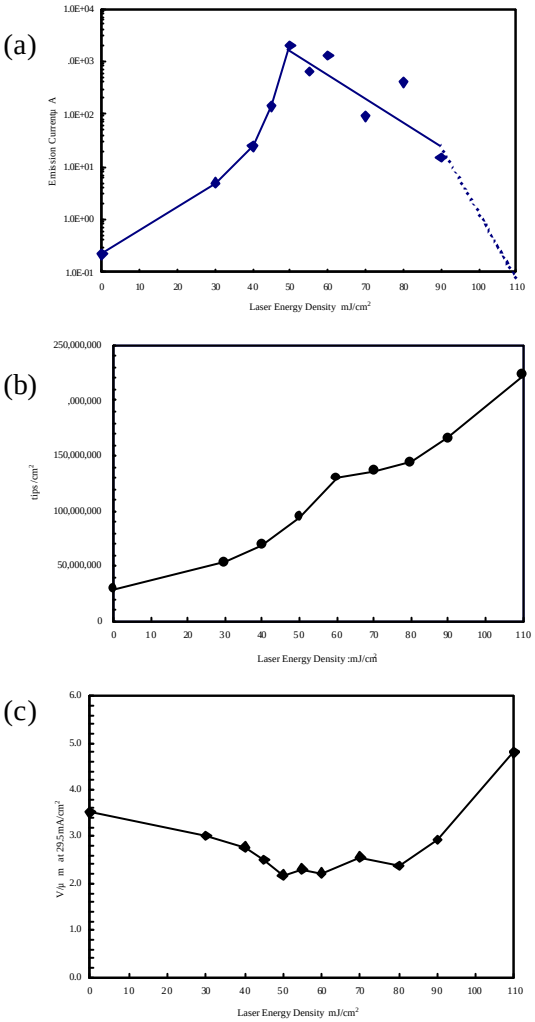

Fig. 10. (a) Emission current as a function of the laser energy density under constant voltage. Applied voltage is 660V. (b) Density of CNT tips as function of laser energy density, and (c) electric field required to obtain a constant emission current density (29.5 mA/cm^2) as a function of laser energy density. Emission measurement was performed with anode-emitter spacing of 0.3 mm.

Figure 10 (a) shows emission current at a constant voltage of 660V as a function of a laser energy density, indicating that the current increased rapidly after laser irradiation up to 50 mJ/cm^2 while it turned to decrease over 60 mJ/cm^2. Figures 11 shows two-dimensional distributions of FE current at 700 V from the CNT-covered honeycomb grids before and after laser irradiation of 45 mJ/cm^2, respectively. Emission area giving current density over 1 mA/cm^2 is displayed in the figures. In Fig. 11 (b), the honeycomb pattern is clearly observed over the whole area, indicating that the FE is uniform and the emitting area is increased several times by the laser irradiation compared with that before irradiation (Fig. 11 (a)).

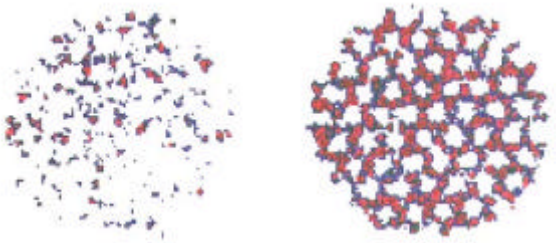

(a) (b)

Fig. 11. Areal distribution of electron emission from the patterned CNT electrode (a) before the laser irradiation and (b) after the irradiation with energy density 45 mJ/cm^2. Emission area giving current density over 1 mA/cm^2 is displayed.

The CNT tips created by laser irradiation had sharp edges and clean surfaces, which would facilitate electron emission. At the same time, the emitting area increased up to several times than the initial one, indicating the increase in the number of emission sites. The increase in the emission current and in the site density observed for laser energy up to 60 mJ/cm^2 is presumably due to the CNT networked structure remaining even after the moderate laser irradiation and the increase in the number of CNT tips created by irradiation. The network structure of CNT layers is considered to be important to maintain a uniform electric field over the cathode surface.

For laser energy over 60 mJ/cm^2, the emitting area turned to decrease in spite of the increase of the tip number. This would be due to the coarsening of the networked structure and the coalescence of created tips at large laser energy. The disruption of network structures and the bunching of CNT tips may bring about electric-field-localization onto a small numbers of protruding CNTs, and thus the emission site density is reduced and the emission uniformity is degraded. These results suggest that an appropriate mesh-size of the CNT networked structure and the number density of CNT tips are important to obtain uniform emissions of electron at lower voltage.

One of the most important technical issues for manufacturing CNT-FEDs is to realize the surface morphology of CNT layers enabling uniform electron emission at lower applied voltage. Figure 10 (c) shows the electric field required to obtain a certain emission current density (29.5 mA/cm^2) as a function of laser energy density. The required electric field decreases down to the minimum value of 2.2 V/μm at 50-60 mJ/cm^2, where the emission uniformity is also the most effectively improved.

5. Acknowledgements

We acknowledge financial supports from the Ministry of Education, Science, Sports and Culture (Grants-in-Aids for Scientific Research (B), and Cooperation of Innovative Technology and Advanced Research in Evolution Area (City Area) Project) and from the NEDO project of "CNT-FED Technology Development".

6. References

[1] Y. Saito and S. Uemura, Carbon **169** (2000).
[2] S. Uemura et al., J. SID **11**, 145 (2003).
[3] C. G. Lee et al., SID02 Digest, pp. 1125-1127 (2002).
[4] J. Dijon et al., SID04 Digest, pp. 820-823 (2004).
[5] Y. Wei, C. Xie, K. A. Dean and B. F. Coll, Appl. Phys. Lett. **79**, 4527 (2001).
[6] Z. L. Wang, R. P. Gao, W. A. de Heer and P. Poncharal, Appl. Phys. Lett. **80**, 856 (2002).
[7] Y. Saito, T. Nakahira and S. Uemura, J. Phys. Chem. B **107**, 931 (2003).
[8] K. Seko, J. Kinoshita and Y. Saito, Jpn. J. Appl. Phys. **44**, L743 (2005).
[9] S. T. Purcell, P. Vincent, C. Journet and V. T. Binh, Phys. Rev. Lett. **88**, 105502-1 (2002).
[10] J. Yotani et al., Jpn. J. Appl. Phys. **43**, L1459 (2004).
[11] J. Kai, M. Kanai, M. Tama, K. Ijima and Y. Tawa, Jpn. J. Appl. Phys. **40**, 4696 (2001).